Vol 11 No 10, October 2002
1009-1963/2002/11(10)/1076-06

Chinese Physics

© 2002 Chin. Phys. Soc.
and IOP Publishing Ltd

Numerical analysis of the mechanism of carrier transport in organic light-emitting devices*

Peng Ying-Quan(彭应全)[a)†], Zhang Fu-Jia(张福甲)[a)], Tai Xi-Shi(台夕市)[b)], He Xi-Yuan(何锡源)[a)], and Zhang Xu(张 旭)[c)]

[a)] *School of Physical Science and Technology, Lanzhou University, Lanzhou 730000, China*
[b)] *School of Chemistry and Chemical Industry, Lanzhou University, Lanzhou 730000, China*
[c)] *Department of Physics, Gansu Institute of Education, Lanzhou 730030, China*

(Received 8 April 2002; revised manuscript received 10 June 2002)

The mechanism of carrier transport in organic light-emitting devices is numerically studied, on the basis of trapped-charge-limited conduction with an exponential trap distribution. The spatial distributions of the electrical potential, field and carrier density in the organic layer are calculated and analysed. Most carriers are distributed near the two electrodes, only a few of them are distributed over the remaining part of the organic layer. The carriers are accumulated near the electrodes, and the remaining region is almost exhausted of carriers. When the characteristic energy of trap distribution is greater than 0.3 eV, it leads to a reduction of current density. In order to improve the device efficiency, organic materials with minor traps and low characteristic energy should be chosen. The diffusion current is the dominant component near the injection electrode, whereas the drift current dominates the remaining region of the organic layer.

Keywords: organic light-emitting device, carrier transport, numerical analysis
PACC: 7860F, 7280L, 0260, 7360R

1. Introduction

In the past decades, organic light-emitting devices (OLEDs) have been widely investigated.[1−4] Since the report of a multiple layer OLED, many new organic luminescent materials have been synthesized,[1−4] and numerous device structures[5−10] and methods for improving quantum efficiency[11−13] have been investigated. Monochromatic OLEDs for display applications are even commercialized. In order to improve the device characteristics, the role of the charge transport mechanism and the organic interface in controlling the device operation need to be further investigated. Both injection-dominated and bulk-dominated mechanisms have been proposed to describe the rate-limiting process in the current–voltage behaviour of OLEDs.

Experimental results show that the transport of the charge carriers in the organic layer (Fig.1) can be described by the trapped-charge-limited conduction with an exponential trap distribution.[14−16] We report on the results of a numerical analysis of the spatial distributions of the carrier density, electric field, electric potential, drift and diffusion currents in the organic layer, as well as on the current–voltage behaviour of single-layer OLEDs (Fig.1).

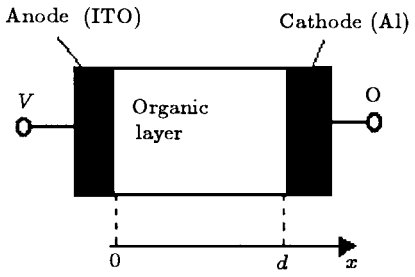


Fig.1. The structure of a single-layer OLED.

2. Numerical model

Organic luminescent materials generally have poor electrical conductivity with a carrier mobility ranging from 10^{-3} to 10^{-8}cm^{2}V^{-1}s^{-1}. Most of them, for example poly(phenylene vinylene) (PPV), are hole-conducting materials, which have much better conductivity for holes than for electrons, and the mobility for holes is generally two orders of magnitude larger than that for electrons.[17] The charge transport in organic luminescent materials is in fact an electric-field-driven chain of redox processes involving neutral molecules or groups and their charged derivatives: anion radicals in the case of electron transport and cation radicals in the case of hole transport. It is the ease of

*Project supported by the National Natural Science Foundation of China (Grant No 60076023).
†Author to whom correspondence should be addressed. E-mail:yqpeng@lzu.edu.cn

formation and stability of the radical cations that is responsible for the much better conductivity for holes than for electrons in many organic luminescent materials. Therefore, the contributions of electrons to the current are negligible in many cases. The following discussion is based on the single-layer OLEDs made of hole-conducting organic luminescent materials, but the results are also valid for OLEDs made of electron-conducting materials, when the charge, density and mobility of holes are replaced by those of electrons. The electric potential ϕ, field F, total hole density p and current density j at a position x in the organic layer are related to one another through the following equations (Fig.1)

$$\frac{\mathrm{d}F}{\mathrm{d}x} = \frac{qp}{\varepsilon_0\varepsilon_\mathrm{r}} \quad \text{(Poisson equation)}, \tag{1}$$

$$p = p_\mathrm{f} + p_\mathrm{t}, \tag{2}$$

$$j = q\mu p_\mathrm{f} F - Dq\frac{dp_\mathrm{f}}{\mathrm{d}x}, \tag{3}$$

$$F = -\frac{\mathrm{d}\phi}{\mathrm{d}x}, \tag{4}$$

$$D = \frac{\mu k_\mathrm{B} T}{q} \quad \text{(Einstein relation)}. \tag{5}$$

Here q is the charge of holes; ε_0 and ε_r are the permittivity of vacuum and the relative dielectric constant of organic materials respectively; p_f, p_t and p are free hole, trapped hole and total hole concentrations respectively; μ is the hole mobility; D is the diffusion coefficient; and k_B and T are the Boltzmann constant and ambient temperature, respectively. The zero point of coordinate x is located at the interface between the anode and the organic layer. According to the theory of the trapped-charge-limited conduction with an exponential trap distribution, the trap density in the organic layer is distributed in energy as follows[17]

$$h(E_\mathrm{t}) = \frac{H_\mathrm{t}}{k_\mathrm{B}Tl}\mathrm{e}^{-E_\mathrm{t}/k_\mathrm{B}Tl}, \tag{6}$$

where E_t is the energy of traps respective to the energy of the highest occupied molecular orbit (HOMO), and $h(E_\mathrm{t})$ is the density of trap states per unit energy in the vicinity of energy E_t. l is the characteristic parameter of the trap distribution, which is defined as the ratio of the characteristic energy E_tc of trap distribution to thermal energy $k_\mathrm{B}T$, i.e. $l = E_\mathrm{tc}/k_\mathrm{B}T$. So l is in fact a measure of the mean trap energy in units of thermal energy. The greater the value of l, the deeper the traps, and vice versa. H_t is the total density of traps, which can be obtained by integrating the product of $h(E_\mathrm{t})$ and the proper Fermi–Dirac distribution function over the trap energies in the range $[E_\mathrm{HOMO}, -\infty]$. In organic semiconductors, the concentration of free charges ρ_f is generally much smaller than that of trapped charges ρ_t, and they are related to one another through the following equations[18]

$$\rho_\mathrm{f} = \theta\rho^l, \tag{7}$$

$$\rho = qp, \tag{8}$$

$$\rho_\mathrm{f} = qp_\mathrm{f}, \tag{9}$$

$$\theta = qN_0\left(\frac{\sin(\pi/l)}{qH_\mathrm{t}(\pi/l)}\right)^l. \tag{10}$$

Substituting Eqs.(8)–(10) into Eq.(7), we obtain

$$p_\mathrm{f} = N_0\left(\frac{\sin(\pi/l)}{H_\mathrm{t}(\pi/l)}\right)^l p^l. \tag{11}$$

For the convenience of developing formulae, dimensionless quantities γ, E, u, s and i, which are the reduced charge density, reduced electric field, reduced voltage, reduced position and reduced current density, respectively, are defined as follows

$$\gamma = \frac{qd^2}{\varepsilon_0\varepsilon_\mathrm{r}k_\mathrm{B}Tl}\rho, \tag{12}$$

$$E = \frac{qd}{k_\mathrm{B}Tl}F, \tag{13}$$

$$\psi = \frac{q}{k_\mathrm{B}Tl}\phi, \tag{14}$$

$$u = \frac{q}{k_\mathrm{B}Tl}V, \tag{15}$$

$$s = \frac{x}{d}, \tag{16}$$

$$i = \left(\frac{q}{k_\mathrm{B}Tl}\right)^{l+1}\frac{d^{2l+1}}{\mu\theta(\varepsilon_0\varepsilon_\mathrm{r})^l}j. \tag{17}$$

Here d is the thickness of the organic layer. The values of reduced position s are between 0 and 1.0.

Substituting Eqs.(5), (7), (13) and (17) into Eq.(3), we have

$$i = E\gamma^l - \gamma^{l-1}\frac{\mathrm{d}\gamma}{\mathrm{d}s}, \tag{18}$$

$$\frac{\mathrm{d}E}{\mathrm{d}s} = \gamma. \tag{19}$$

For the convenience of simplifying the above equations, dimensionless variables z and y are defined as

$$z = i^{-\frac{1}{2l+1}}E, \tag{20}$$

$$y = i^{-\frac{2}{2l+1}}\gamma. \tag{21}$$

Substituting these into Eqs.(18) and (19), we have

$$\frac{\mathrm{d}y}{\mathrm{d}z} = z - \frac{1}{y^l}. \tag{22}$$

When $y \to \infty$, the above equation becomes

$$\frac{\mathrm{d}y}{\mathrm{d}z} = z, \tag{23}$$

i.e.

$$y = \frac{1}{2}z^2 + \text{const or } z = \pm\sqrt{2y + \text{const}} \text{ for } y \to \infty. \tag{24}$$

Thus, we have $z \to \pm\infty$, when $y \to \infty$. It is easy to see from Eq.(20) that the reduced field E is proportional to z, if the reduced current density i is kept constant. Thus we have $E(0) = -\infty$ and $E(1) = +\infty$. It can be seen from Eq.(22) that y has a minimum value $y_\mathrm{p} = z_\mathrm{p}^{-1/l}$ at $z = z_\mathrm{p}$, and we will see later that y_p corresponds to the operation voltage V at a constant value of l. Equation (22) is solved by using standard numerical methods with the coordinates of the point (z_p, y_p) as starting values. The spatial distributions of the reduced electric field E and the reduced charge density γ can be calculated from Eqs.(20) and (21) by using the values of z and y. From Eqs.(4) and (14) we have the spatial distribution of the reduced electric potential

$$\psi(s) = -\int_0^s E(s')\mathrm{d}s'. \tag{25}$$

With the help of Eqs.(13) and (14), the distributions of the electric field F and potential ϕ can be calculated. From Eqs.(19) and (21), we have

$$\int_0^1 \mathrm{d}s = \int_{-\infty}^{\infty} \frac{\mathrm{d}E}{\gamma} = i^{-\frac{1}{2l+1}} \int_{-\infty}^{\infty} \frac{\mathrm{d}z}{y} = 1, \tag{26}$$

$$i = \left(\int_{-\infty}^{\infty} \frac{\mathrm{d}z}{y} \right)^{2l+1}, \tag{27}$$

from which the reduced current density i can be calculated. In order to gain the expression for the reduced voltage u, Eq.(18) is rewritten as

$$\frac{i}{y^l} = E - \frac{\mathrm{d}(\ln\gamma)}{\mathrm{d}s}, \tag{28}$$

and is then integrated on both sides of the equation separately. With the help of Eqs.(13), (15), (19) and (21), we have

$$i\int_0^1 \frac{\mathrm{d}s}{\gamma^l} = u - \ln\left(\frac{\gamma(1)}{\gamma(0)}\right), \tag{29}$$

$$u = \int_{-\infty}^{\infty} \frac{\mathrm{d}z}{y^{l+1}} + \ln\left(\frac{\gamma(1)}{\gamma(0)}\right). \tag{30}$$

It is easy to see from $V(j = 0)$=0 that $\ln(\gamma(1)/\gamma(0))$=0. Thus we have

$$u = \int_{-\infty}^{\infty} \frac{\mathrm{d}z}{y^{l+1}}. \tag{31}$$

With the help of Eqs.(15) and (17), the function of current density j with the operation voltage V can be calculated.

3. Results and discussion

The numerical solutions to Eq.(22) are shown in Fig.2 for l=2 and z_p=10.0, in which y decreases from about 50.0 to nearly 5.0 as z increases from –10.0 to –2.0, and decreases very slowly in the range $-2.0 < z < 10.0$, reaching a minimum value of about 0.1 at z=10.0. Within the range $z > 10.0$, y increases rapidly.

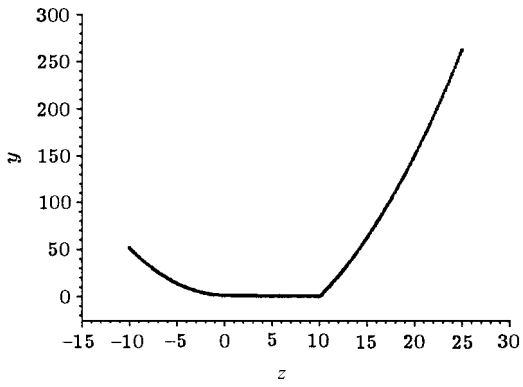


Fig.2. The calculated y–z curve for l=4.0 and z_p=10.0.

Figure 3 shows the spatial distributions of the reduced charge density γ, reduced electric field E and reduced potential ψ for different values of l. For a given l (e.g. l=4.0), the reduced charge density decreases with the reduced position rapidly from a very high value to about 5×10^2 near the anode ($0 < s < 0.1$), and decreases then very slowly in the middle range ($0.1 < s < 0.98$), reaching a minimum at about 0.98 (Fig.3(a)). It then increases rapidly near the cathode ($0.98 < s < 1.0$), which is caused by the very low electric potential (see Fig.4(b)). The reduced electric field E increases monotonically with the reduced position s, which varies sharply near the cathodes and slowly in the rest of the region. The reduced potential ψ decreases monotonically with the reduced position s, and the larger the value of l, the greater the rate of decrease. For a given position in the middle region, the reduced charge density and the reduced electric field

decrease with l, and the middle region will be almost exhausted of carriers when l is very large (e.g. $l > 12$).

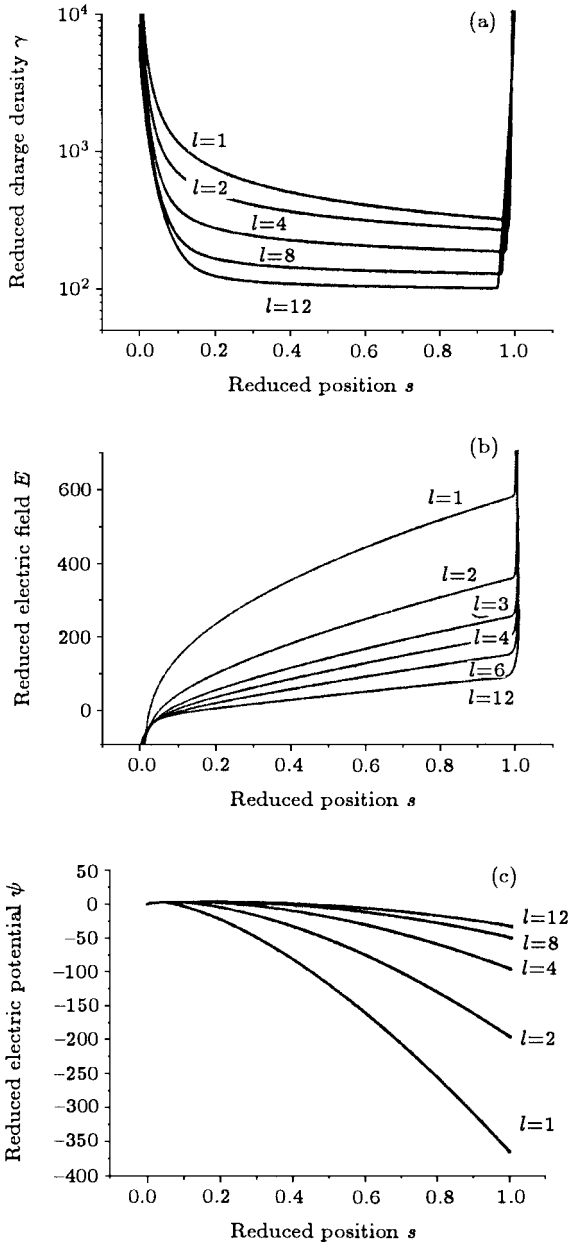


Fig.3. Spatial distributions of (a) reduced charge density, (b) reduced electric field, and (c) reduced potential.

The spatial distributions of the electric field, potential, carrier density and current density for a typical single-layer OLED are shown in Figs.4 and 5. The electric field F increases monotonically with the reduced position s, which is rapid near the electrode (s <0.05 and s >0.95), and slowly and nearly linearly in the middle range ($0.05 < s < 0.95$). It tends to be $-\infty$ at the anode and $+\infty$ at the cathode. But this is not possible in a real physical device, because on the one hand, there are interfacial states in the interface between the electrodes and the organic material, which neutralize part of the charges near the electrodes and decrease the electric field there. On the other hand, both the hole density at the anode and the electron density at the cathode have only limited values, thus only limited charges can be injected into the organic material, which can only produce limited electric fields at the electrodes. The larger l is, the more rapid the increase near the electrodes, and the more slow the increase of the electric field in the middle range.

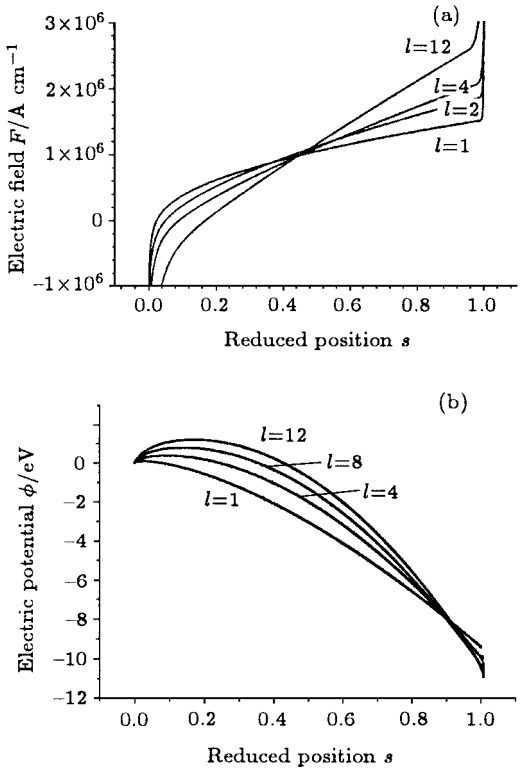


Fig.4. The calculated (a) electric field and (b) electric potential for different values of l, with the selected parameters of d=100nm, T=300K, N_0=1.0×10^{20}cm^{-3}, H_t=1.0×10^{20}cm^{-3}, l=2.0, V=10.0V.

For a given value of l (e.g. l=4), the electric potential ϕ increases with the reduced position for s less than about 0.1 until it reaches a maximum. Then it decreases with s for larger values of s, and reaches a minimum value at the cathode, which causes an accumulation of free and trapped holes near the cathode. The distributions of free holes and trapped holes are similar (Fig.5(a)); they decrease near the anode and increase near the cathode very rapidly, and decrease very slowly in the middle region of the organic layer. When the value of l rises from 2.0 to 3.0, or the characteristic energy of the trap distribution E_{tc} rises from 0.05 to 0.075eV, the concentration of free holes in the middle region reduces to only about one per cent of

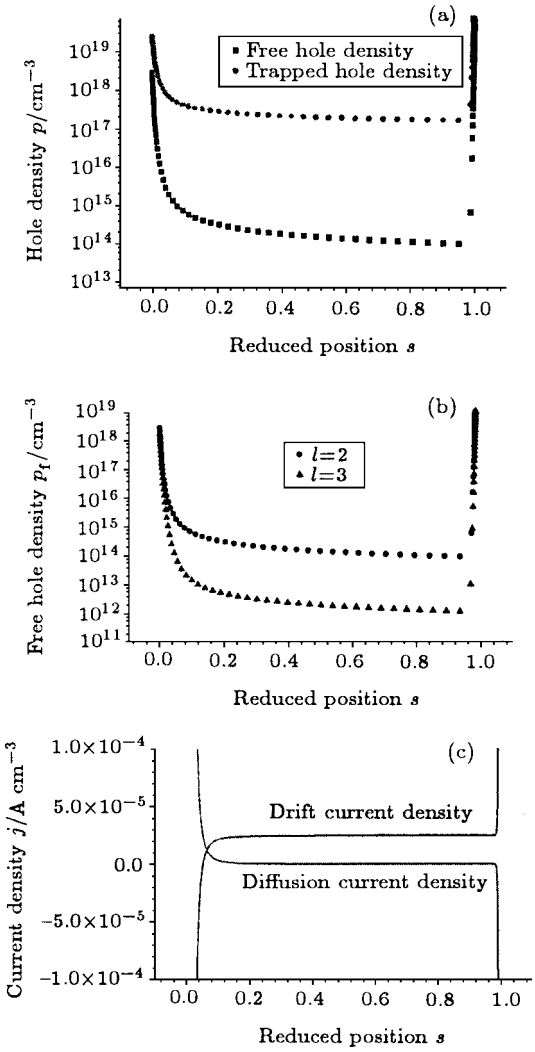


Fig.5. The distribution of charge densities and current densities, with the selected parameters of d=100nm, T=300K, N_0=1.0×10^{20}cm^{-3}, H_t=1.0×10^{20}cm^{-3}, l=2.0, and V=10.0V: (a) a comparison between the density distributions of the free and trapped holes; (b) the distributions of the free holes for l=2 and 3; (c) the distributions of the drift and the diffusion currents.

the original value (Fig.5(b)). Thus, for greater values of l (e.g. $l > 12$ or E_{tc} >0.3eV at room temperature), free charges will be accumulated at the regions near the electrodes, and the middle region is finally exhausted, which leads to a high turn-on voltage and a poor device efficiency. Thus, organic luminescent materials with low trap density and low characteristic energy in trap distribution should be chosen, in order to decrease the turn-on voltage and to improve the quantum efficiency. The absolute values of the drift current and diffusion current are very large near the electrodes, but with opposite directions (Fig.5(c)). Diffusion current dominates near the anode, despite the fact that the drift current dominates the other regions. In the middle region, the drift current is almost five orders of magnitude larger than the diffusion current, and is almost a constant.

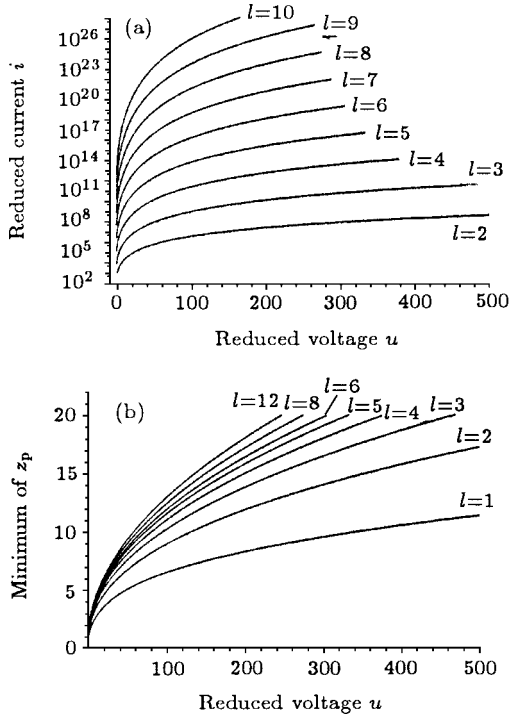


Fig.6. The calculated i–u (a) and z_p–u (b) curves.

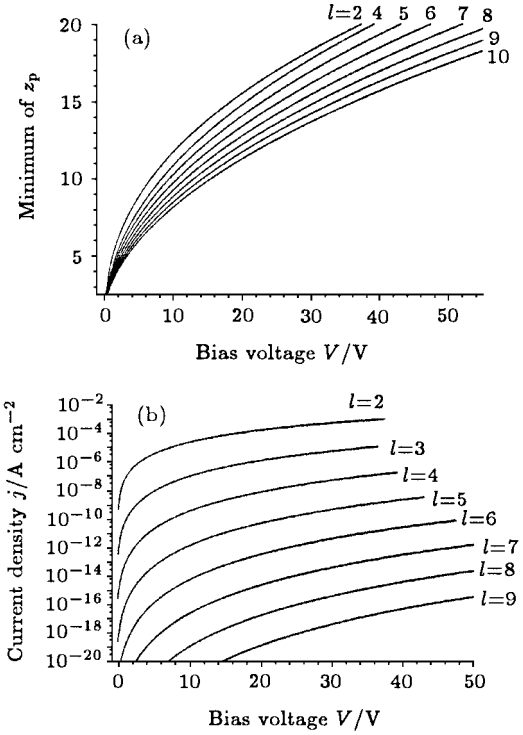


Fig.7. The calculated z_p–V and j–V curves, with the selected parameters of d=100nm, T=300K, μ=1.0×10^{-6}cm^2 V^{-1} s^{-1}, N_0=1.0×10^{20} cm^{-3}, H_t=1.0×10^{20} cm^{-3}, ε_r=2.0.

The values z_p and i increase with the reduced voltage u monotonically at a constant l value, and

the larger the value of l, the greater the rate of increase of z_p in the z_p–u curve, and the smaller the rate of increase in the i–u curve (Fig.6(a)). Both z_p and j increase with the operation voltage V for a constant value of l (Fig.7). The larger the value of l, the smaller the rate of increase of z_p. The j–V curve increases quickly at operation voltages less than about 2.0V, and gradually slows as V increases.

4. Summary

The spatial distributions of the electric potential, electric field and carrier density in single-layer OLEDs are numerically analysed. Most free and trapped charges are located near the electrodes, only a small amount is located in the middle region of the organic layer, when the characteristic trap energy is high. The electric field is nearly linearly distributed in the bulk of the organic layer. The diffusion current dominates near the injection electrode, and the drift current dominates the remaining part of the organic layer. In the middle region, the diffusion current is several orders of magnitude smaller than the drift current.

References

[1] Slooff L H, Polman A, Cacialli F, Friend R H *et al* 2001 *Appl. Phys. Lett.* **78** 2122

[2] Hu W P, Matsumura M, Wang M Z *et al* 2000 *Japan. J. Appl. Phys.* **39** 6445

[3] List E J W, Leising G, Schulte N *et al* 2000 *Japan. J. Appl. Phys.* **39** L760

[4] Pandey S S, Takashima W, Nagamatsu S *et al* 2000 *Japan. J. Appl. Phys.* **39** L94

[5] Fournet P, Coleman J. N, Lahr B *et al* 2001 *J. Appl. Phys.* **90** 969

[6] Yang X H, Mo Y Q, Yang W *et al* 2001 *Appl. Phys. Lett.* **79** 563

[7] Thompson J, Blyth R I R, Mazzeo M *et al* 2001 *Appl. Phys. Lett.* **79** 560

[8] Wilkinson C I, Lidzey D G, Palilis L C *et al* 2001 *Appl. Phys. Lett.* **79** 171

[9] Michio M and Takumi F 2001 *Japan. J. Appl. Phys.* **40** 3211

[10] Lmimouni K, Legrand C, Dufour C *et al* 2001 *Appl. Phys. Lett.* **78** 2437

[11] Chen Z J, Yu J S and Sakuratani Y 2001 *J. Appl. Phys.* **89** 7895

[12] Parthasarathy G, Shen C and Kahn A 2001 *J. Appl. Phys.* **89** 4986

[13] Deng Z B, Li S T, Chen L C *et al* 1997 *Acta Phys. Sin.* (Overseas Edition) **6** 921

[14] Campbell A J, Bradley D D C and Lidzey D G 1997 *J. Appl. Phys.* **82** 6326

[15] Campell A J, Weaver M S and Lidzey D G 1998 *J. Appl. Phys.* **84** 6737

[16] Burrows P E, Shen Z, Bulovic V *et al* 1996 *J. Appl. Phys.* **79** 7991

[17] Yang J and Shen J 1998 *J. Appl. Phys.* **83** 7706

[18] Bonham J S and Jarvis D H 1977 *Austr. J. Chem.* **30** 705